Dynamics of the folded and unfolded villin headpiece (HP35) measured with ultrafast 2D IR vibrational echo spectroscopy

Jean K. Chung, Megan C. Thielges, and Michael D. Fayer[1]

Department of Chemistry, Stanford University, Stanford, CA 94305

Contributed by Michael D. Fayer, January 12, 2011 (sent for review January 1, 2011)

A series of two-dimensional infrared vibrational echo experiments performed on nitrile-labeled villin headpiece [HP35-$(CN)_2$] is described. HP35 is a small peptide composed of three alpha helices in the folded configuration. The dynamics of the folded HP35-$(CN)_2$ are compared to that of the guanidine-induced unfolded peptide, as well as the nitrile-functionalized phenylalanine (PheCN), which is used to differentiate the peptide dynamic contributions to the observables from those of the water solvent. Because the viscosity of solvent has a significant effect on fast dynamics, the viscosity of the solvent is held constant by adding glycerol. For the folded peptide, the addition of glycerol to the water solvent causes observable slowing of the peptide's dynamics. Holding the viscosity constant as GuHCl is added, the dynamics of unfolded peptide are much faster than those of the folded peptide, and they are very similar to that of PheCN. These observations indicate that the local environment of the nitrile in the unfolded peptide resembles that of PheCN, and the dynamics probed by the CN are dominated by the fluctuations of the solvent molecules, in contrast to the observations on the folded peptide.

nitrile IR probe | peptide dynamics

The structure of proteins, both folded and unfolded, are inherently dynamic in nature. A protein is constantly undergoing interconversions among a range of structures separated by relatively low energy barriers. Fast conformational sampling can give rise to protein structural evolution on slower time scales. Many experimental and theoretical studies have focused on the native structure due to the relevance of the native state protein to its biological functions, but also because of difficulties associated with characterizing proteins under unfolding conditions, where they can exist in heterogeneous distributions of many conformations (1, 2). Properties of the unfolded state are also significant because they play important roles in folding and stability, transport across membranes, and proteolysis and protein turnover (1). Unfolded proteins have dynamics that are different from the native protein, and the differences in dynamics can shed light on the relationship between the native and the unfolded protein.

An attractive target for studying differences between the folded and unfolded structures is the villin headpiece 35 (HP35), a peptide chain composed of 35 amino acids found in a chicken villin as a small subdomain. HP35 folds fast (~1 μs) compared to large proteins, allowing tractable folding/unfolding simulations. Consequently, it has served as a model system in a number of computational folding studies (3–5), as well as a variety of experimental studies (6–8). NMR and X-ray diffraction studies have indicated that wild-type HP35 folds into three alpha helices (Fig. 1), which encase the hydrophobic core composed of three phenylalanines (9, 10).

In this paper, the results of a series of ultrafast 2D IR vibrational echo experiments on nitrile-incorporated HP35 are presented. Two CN-functionalized phenylalanines were inserted into the hydrophobic core of the peptide where they will be sensitive to peptide dynamics. The ultrafast dynamics of the folded peptide were compared to those of the chemically induced unfolded peptide. In addition, the dynamics of a single amino acid, the nitrile-functionalized phenylalanine (PheCN), were investigated. The amino acid is used to distinguish between dynamics sensed by CN arising from the peptide chain motions versus those of the solvent. The peptide was unfolded using guanidinium hydrochloride (GuHCl). The addition of GuHCl increases the viscosity of the solvent. Therefore, the experiments have been viscosity-controlled; that is, glycerol was added to the solutions, and the amount of glycerol was reduced as GuHCl was added to keep the viscosity constant. The dynamics of HP35 in water versus the water/glycerol solution shows that the viscosity has a substantial effect on the rates of peptide structural motions. The dynamics of HP35 in water as shown by the nitrile 2D IR spectral evolution are much slower than those of PheCN, demonstrating that the nitrile probe is reporting on the structural dynamics of the folded protein rather than on the solvent. The dynamics of the PheCN slow when glycerol is added, but are still much faster than HP35 in the water/glycerol solution. Unfolding the peptide with GuHCl, confirmed by CD measurements, results in time-dependent 2D IR spectra that are very similar to those of the PheCN in the same solvent. This result suggests that unfolding moves the nitrile group from the interior of the folded peptide to the solvent-exposed exterior.

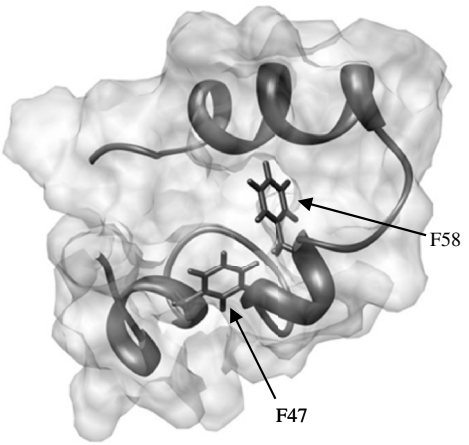

Fig. 1. The NMR structure of wild-type HP35 (PDB ID code 1VII). The phenylalanine residues functionalized with CN (F47 and F58) are shown.

The availability of ultrafast mid-IR laser systems has enabled the application of various time-resolved techniques to biological

Author contributions: J.K.C. and M.D.F. designed research; J.K.C., M.C.T., and M.D.F. performed research; J.K.C. and M.D.F. analyzed data; and J.K.C. and M.D.F. wrote the paper.

The authors declare no conflict of interest.

[1]To whom correspondence should be addressed. E-mail: fayer@stanford.edu.

This article contains supporting information online at www.pnas.org/lookup/suppl/doi:10.1073/pnas.1100587108/-/DCSupplemental.

molecules on very fast time scales that are inaccessible by other means. In particular, 2D IR vibrational echo spectroscopy has proven to be useful in gaining insights into proteins' dynamic nature, which is intimately involved in their functions that occur on much longer time scales (11, 12). Applications of 2D IR spectroscopy in biology include the study of protein dynamics, structure, folding and unfolding, and enzymatic specificities (13–19). These studies provide information on the structure and dynamics of proteins and provide a connection between experimental observations and molecular dynamic simulations in the important subnanosecond time regime (20–22). The nitrile group is a vibrational probe that has been the focus of recent investigations, mainly in time-independent vibrational studies. For time-dependent studies, nitrile can produce reasonable signals, and it is sensitive to the electric field (23). CN is very useful because it can be inserted into many biological molecules via molecular engineering techniques (24, 25). These techniques include the in vivo genetic incorporation of unnatural amino acids developed by Schultz et al., which allows the introduction of CN probes virtually anywhere in a protein (26). Two 2D IR studies have been performed on biological systems using CN as the probe. One study involved HIV reverse transcriptase using a bound substrate containing a CN group (27). The other studied nitrile-labeled HP35 in its native state in water (28). Here we extend the use of nitrile as a probe of dynamics to investigate the effects of unfolding and viscosity on dynamics.

Results and Discussions

A. Circular Dichroism Spectroscopy. To monitor the GuHCl-induced unfolding of HP35-$(CN)_2$, CD spectroscopy was performed on the peptide with varying concentrations of GuHCl. Because the hydrophobic core enclosed by the three alpha helices is believed to play an essential role in the stability of the peptide, it is possible that the incorporation of the nitrile groups into the phenylalanines modifies the native structure. Indeed, the presence of one nitrile group in one phenylalanine (F58) makes the peptide (HP35-P) less stable to urea denaturation (7) when compared to the wild type under similar conditions (29). At 0 M GuHCl, circular dichroism spectra of HP35-$(CN)_2$ show a negative signal at ~220 nm characteristic for alpha helices, suggesting HP35-like folding (see Fig. 2*A*). Fig. 2*B* shows the GuHCl concentration-dependent CD data at 222 nm. Compared to the wild-type peptide, however, the data suggest that HP35-$(CN)_2$ is destabilized, with the transition GuHCl concentration shifting below 4 M (30). The much more gradually increasing sigmoidal profile of unfolding suggests a considerable reduction in cooperativity. For the infrared experiments, GuHCl concentrations of 0, 4, and 6 M were used; judged by the CD spectra, HP35-$(CN)_2$ is expected to be folded at 0 M GuHCl and nearly completely unfolded at 4 and 6 M.

B. Fourier-Transform Infrared Spectroscopy. Fig. 3 shows the IR absorption spectra of the CN stretching modes of the HP35-$(CN)_2$ peptide (*A*) and PheCN (*B*) in the different solvents. The CN stretching modes of HP35-$(CN)_2$ and PheCN are single bands between 2,234 and 2,236 cm^{-1}, which is consistent with other aromatic nitriles (31). In this region of the mid-IR, a water combination (bending and libration) mode occurs; adding GuHCl and glycerol has a beneficial effect of reducing the sloping background. For the folded HP35-$(CN)_2$ in pH 5.0 sodium acetate buffer (0 M GuHCl curve in Fig. 3*A*), the CN stretching mode is a single band at 2,234.5 cm^{-1} with the FWHM of 13.6 cm^{-1}. Although there are two nitrile probes in each HP35-$(CN)_2$ peptide, the FTIR spectra show only one Gaussian band in the native state (0 M GuHCl). That a single band is observed despite the presence of two CN probes indicates that the CN environments are very similar. The NMR structure (Fig. 1) is consistent with this

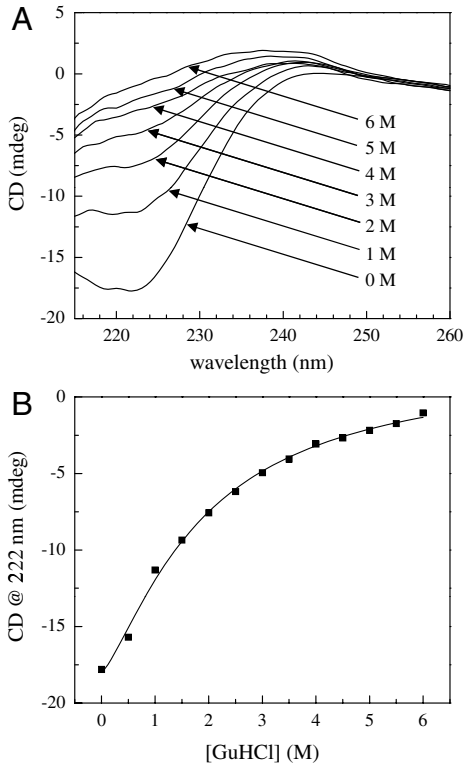

Fig. 2. (*A*) CD spectra collected at several GuHCl concentrations, showing signals characteristic of alpha helices at ~220 nm. (*B*) GuHCl titration curve obtained from CD data, monitored at 222 nm.

observation, as the phenylalanine residues on which the probes are bound are packed closely together in the hydrophobic core.

When the peptide is unfolded in 6 M of GuHCl, there is a single somewhat narrower (FWHM 13.0 cm^{-1}) band, shifted slightly to a lower frequency compared to the folded peptide. This obser-

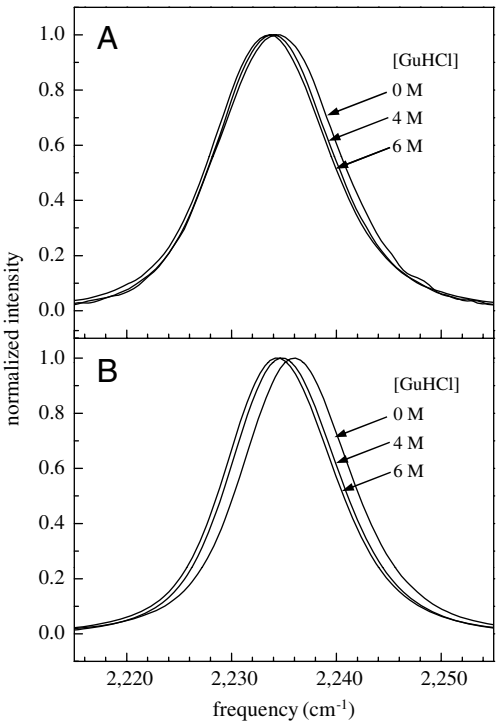

Fig. 3. Normalized FT IR spectra of (*A*) HP35-$(CN)_2$ and (*B*) PheCN at various GuHCl concentrations. See Table 1 for the summary of FTIR fit parameters.

vation implies that the environments around the two CN probes are still essentially the same. The FTIR spectrum of PheCN (Fig. 3*B*) shows a similar shift to a lower frequency in a 6 M GuHCl solution when compared to 0 M GuHCl, but the linewidth remains unchanged. It can be inferred, therefore, that the increased ionic content due to GuHCl causes the shift in frequency, but the unfolding of the peptide is responsible the small change in linewidth.

At denaturing GuHCl concentrations, the viscosity of solvent is significantly increased (32). Because viscosity of the solvent can affect the fast dynamics of the molecules of interest (33), it was controlled by adjusting the glycerol content in each sample. The addition of glycerol to the 0 M GuHCl solutions had no significant effect on the FTIR spectra.

Peptide concentration studies showed that caution has to be taken to avoid the appearance of a shoulder due to aggregation of the peptide when the concentration is too high. In the work by Urbanek et al. (28), the HP35 phenylalanine (F58) is labeled with CN (HP35-P). However, the spectrum in water-buffer solution consisted of two bands, one at 2,234.5 cm^{-1} and another at 2,228.7 cm^{-1}, in contrast to the 0 M spectrum shown in Fig. 3*A*. The authors speculated that the bands corresponded to two conformational states of HP35-P in which the CN senses either a hydrophobic or a hydrophilic environment, respectively. According to our observations, however, the lower frequency band is most likely due to aggregation of peptide. Aggregation is discussed further in *SI Text* including IR spectra that show that the appearance of the second band is a consequence of high concentration.

C. Two-Dimensional Infrared Vibrational Echo Spectroscopy. In the 2D IR experiments (34), the mid-IR pulses are split into multiple beams, three of which are crossed at the sample. The delay time between pulses 1 and 2 is τ and between pulses 2 and 3 is T_w. The vibrational echo signal is emitted following the third pulse at a time $\leq\tau$ in a unique direction. The vibrational echo is combined with another pulse, called the local oscillator, which provides heterodyne detection and phase information. The heterodyned vibrational echo signal is then dispersed by a monochromator and detected by a 32-element mercury–cadmium–telluride detector. Each element of the detector records an interferogram that yields the ω_m (vertical axis) in the 2D spectrum. Scanning τ produces a time domain interferogram at each ω_m. These interferograms are Fourier transformed and yield the ω_τ (horizontal) axis of the 2D spectrum. In the experiments, τ is scanned for fixed T_w to produce a 2D IR spectrum. T_w is then changed, and τ is again scanned to give another 2D IR spectrum. The change in the spectra with T_w provides the dynamic information.

The theory, analysis, and interpretation of 2D IR vibrational echo spectroscopy used here have been presented in full detail previously (35–37). As the time T_w is increased, the peptides have more time to sample different structural configurations. As a peptide's structure evolves, the frequency of the CN stretch changes within the distribution of frequencies reflected by the inhomogeneously broadened absorption spectrum. This frequency evolution is called spectral diffusion, and it is directly related to the conformational fluctuations of the peptide. Simulations of myoglobin-CO have shown that inhomogeneous broadening and spectral diffusion are caused by the Stark effect (38, 39). Structural fluctuations of the protein and the solvent produce a time-dependent electric field at the vibrational reporter, which is CO for myoglobin-CO and CN in the present case. The structural dynamics induced time evolution of the electric field produces spectral diffusion. The time dependence of the spectral diffusion was extracted from the 2D IR spectra using the center line slope (CLS) formalism (35, 36). The CLS method quantifies the time-dependent changes in two-dimensional line shapes and is used to obtain the frequency–frequency correlation function (FFCF). The CLS is a normalized function that is closely related to the FFCF. Its decay times are the same as those in the FFCF. The difference between 1 and the value of the CLS at $T_w = 0$ is related to the homogeneous component. Combining the CLS with the linear absorption spectrum yields the full FFCF. The FFCF is the direct connection between the experimental observables and the details of the dynamics and structure of the system. The FFCF for proteins have been calculated using molecular dynamics simulations (21, 22).

The multiexponential form of the FFCF, $C(t)$, was used to model the FFCF (35–37):

$$C(t) = \sum_{i=1}^{n} \Delta_i^2 e^{-t/\tau_i} + \Delta_s^2.$$

For the ith dynamical process, Δ_i is the range of CN frequencies sampled due to fluctuations of the CN environment, and τ_i is the time constant of these fluctuations. The static term Δ_s represents the contribution to the CN frequency distribution that arises from peptide structural interconversions that are so slow that they fall outside the experimental time window, which is limited by the vibrational lifetime. This form of the FFCF has been widely used and found applicable in studies of the structural dynamics of proteins (22, 37, 40, 41). In this study, the functional form of two exponential terms, one of which is motionally narrowed, plus the static term were sufficient to describe the FFCF obtained from fittng the CLS data. If $\Delta_i\tau_i < 1$, the dynamics are motionally narrowed and contribute to the homogeneous linewidth. The motionally narrowed dynamics are characterized by $T_2^* = 1/\Delta^2\tau$, where T_2^* is the pure dephasing time. The total homogeneous dephasing time, T_2, is determined by $\frac{1}{T_2} = \frac{1}{T_2^*} + \frac{1}{2T_1} + \frac{1}{3T_{or}}$. T_1 is the vibrational lifetime (4.5 ps), which was measured independently by pump–probe spectroscopy, and T_{or} is the orientational relaxation time. T_{or} was omitted because it is so long for both the peptide and PheCN that it makes a negligible contribution. The pure dephasing linewidth is $\Gamma = 1/\pi T_2^*$.

Fig. 4 displays a few of the 2D IR spectra of HP35-$(CN)_2$ and PheCN in different solvents at short T_w (0.4 ps). Greater elongation of a spectrum along the diagonal reflects greater inhomogeneity of the dynamic line at the particular T_w. By comparing

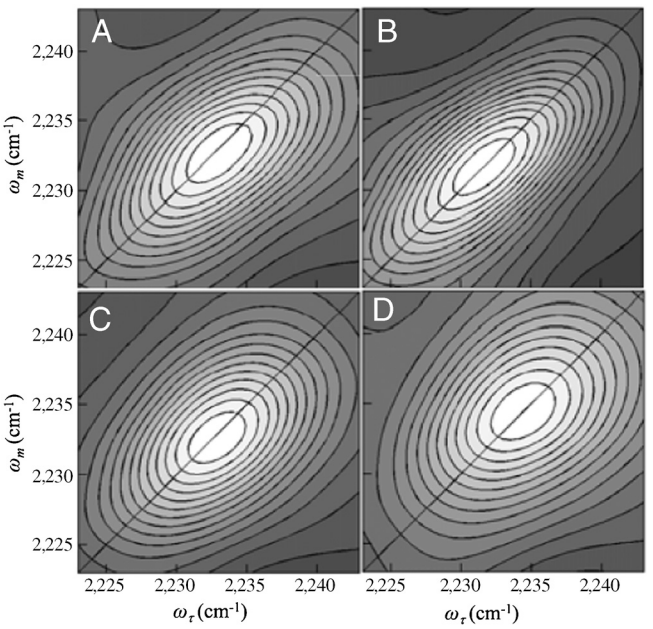

Fig. 4. Two-dimensional IR spectra of (*A*) native HP35-$(CN)_2$ in water; (*B*) native HP35-$(CN)_2$ in water/glycerol solution (viscosity—2.7 cP); (*C*) unfolded in 6 M GuHCl (viscosity—2.7 cP); (*D*) PheCN in water/glycerol solution (viscosity—2.7 cP), all at the waiting time $T_w = 0.4$ ps.

Figs. 4 *A* and *B*, the native peptide in water and in water/glycerol, respectively, it is clear that the increase in viscosity by the addition of glycerol significantly changes the dynamics. Fig. 4*C* is the peptide with 6 M GuHCl and the same viscosity as used for the data in Fig. 4*B*. The change in the spectrum is obvious and indicates that the dynamics reported by the CN spectral diffusion are much faster. The CD data (Fig. 2*B*) show that the peptide is denatured at this GuHCl concentration. Fig. 4*D* is the data for the single amino acid, PheCN, in water/glycerol solution with the same viscosity as the solutions used for Fig. 4 *B* and *C*. The spectrum in Fig. 4*D* is very similar to that in Fig. 4*C*.

The corresponding CLS data and fits are shown in Fig. 5. The FFCF parameters obtained from the fits to the CLS data and the linear absorption spectra are given in Table 2. Fig. 5*A* shows a comparison of the folded peptide in water (filled circles), in water/glycerol (diamonds), which increases the viscosity, and the CN labeled amino acid, PheCN, in water (squares). First, comparing the peptide in water to PheCN in water shows that the dynamics experienced by the CNs in the core of the peptide are much slower than those of the CN when it is bound to a single amino acid and exposed to the water solvent. The curves are borne out by the FFCF parameters in Table 2. Compared to HP35 in water, the FFCF of PheCN in water has a much shorter decay constant τ_1 and no static component; that is, $\Delta_s = 0$. The FFCF of HP35 has a longer decay constant and a significant static component, which means that there are slower dynamics outside of the experimental time window of ~10 ps. These results are consistent with the CNs on HP35 being buried in the hydrophobic core of the peptide, with dynamics determined mainly by the motions of the peptide. These FFCF values in Table 2 for HP35-$(CN)_2$ are not the same as those of HP35-P obtained by Urbanek et al. (28). As mentioned above and discussed in

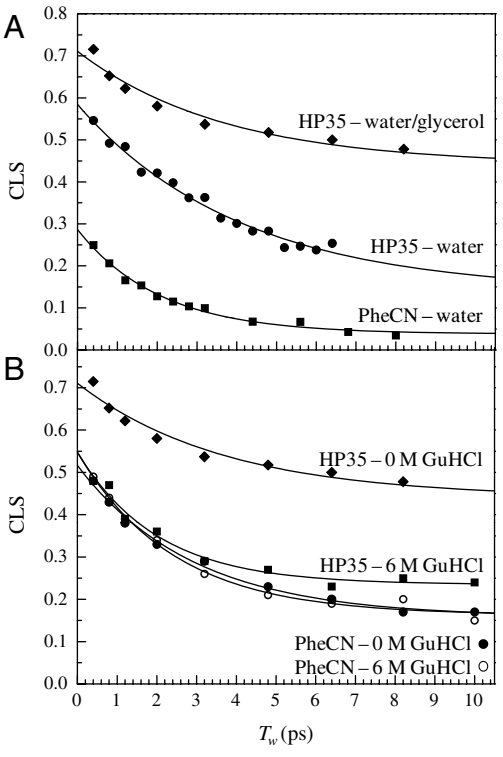

Fig. 5. CLS data (points) and exponential fits (solid curves) for (*A*) HP35-$(CN)_2$ in water/glycerol solution (diamonds; viscosity—2.7 cP), in water (filled circles; viscosity—1 cP), and PheCN in water (squares; viscosity—1 cP); (*B*) HP35-$(CN)_2$ in water/glycerol solution with 0 M GuHCl (diamonds; viscosity—2.7 cP), HP35-$(CN)_2$ with 6 M GuHCl (squares; viscosity—2.7 cP), PheCN in water/glycerol solution, 0 M GuHCl (filled circles; viscosity—2.7 cP), and PheCN in with 6 M GuHCl (open circles; viscosity—2.7 cP).

Table 1. FTIR parameters for HP35-$(CN)_2$ and PheCN

	[GuHCl] (M)	Center (cm^{-1})	FWHM (cm^{-1})
HP35	0	2234.4 ± 0.2	13.6 ± 0.2
	4	2234.0 ± 0.2	13.0 ± 0.2
	6	2233.8 ± 0.2	13.0 ± 0.2
PheCN	0	2236.3 ± 02	12.2 ± 02
	4	2235.2 ± 02	12.2 ± 02
	6	2234.8 ± 02	12.2 ± 02

SI Text, the differences probably arise from aggregation in the HP35-P sample, which led to fitting the 2D IR spectra assuming the existence of two conformational states of the peptide. Structural differences between HP35-P and HP35-$(CN)_2$ might also account for the differences. However, in both cases, the CNs are in the interiors of the folded peptide.

When glycerol is added to the solution bringing the viscosity to 2.7 cP, the dynamics of the peptide slow further (top curve of Fig. 5*A*). In Table 2, data for experiments with glycerol but no GuHCl are listed as 0 M. The main changes upon the addition of glycerol are an increase in the pure dephasing time, T_2^*, and a large increase in the static component. The decrease in Δ_1 and the increase in Δ_s show that a portion of the fluctuations of structures that make up the inhomogeneous absorption line have slowed. However, within experimental error, τ_1 does not change. This is consistent with observations on much larger globular heme proteins, such as myoglobin-CO and hemoglobin-CO, which display weak dependences of the fast dephasing times on viscosity (42).

As discussed above, glycerol was added as necessary to keep the viscosity constant as GuHCl was added. For fixed viscosity, the concentration of glycerol itself does not seem to alter the dynamics, as the CLS data for unfolded HP35-$(CN)_2$ are the same whether it is in 4 M GuHCl/14% glycerol or 6 M GuHCl/10% glycerol solvent (both have the viscosity of 2.7 cP).

Fig. 5*B* shows the effect of unfolding the peptide on the dynamics sensed by the CN probe. The top curve of Fig. 5*B* (diamonds) is the same as the top curve in Fig. 5*A*. Upon addition of 6 M GuHCl, with the viscosity held constant, the decay (squares) becomes much faster. From Table 2 it is seen that unfolding the peptide results in a faster pure dephasing time, almost a factor of 2 decrease in the decay time constant, τ_1, and a smaller static component, Δ_s. Thus, unfolding has a major influence on the dynamics sensed by the CN probe. Within experimental error, the dynamics are the same for the peptide in 4 and 6 M GuHCl (see Table 2). The large change in the dynamics in going from the folded peptide to the unfolded peptide is in contrast to the linear absorption spectrum, which shows very little change (see Fig. 3*A*).

Fig. 5*B* also shows the CLS curves for PheCN in 0 M (filled circles) and 6 M GuHCl (open circles). These solutions have the same viscosities. Within experimental error the data for PheCN in 4 M GuHCl is the same (see Table 2). The PheCN dynamics do not depend on the GuHCl concentration but depend strongly on the viscosity as can be seen by comparing the PheCN data in Fig. 5 *A* and *B* and in Table 2. Of particular note is that the HP35 data in 6 M GuHCl and the PheCN data of the same

Table 2. FFCF parameters for HP35-$(CN)_2$ and PheCN

Sample	Γ (cm^{-1})	T_2^* (ps)	Δ_1 (cm^{-1})	τ_1 (ps)	Δ_s (cm^{-1})
HP35 water	4.4 ± 0.4	2.4 ± 0.2	3.9 ± 0.1	4.1 ± 0.8	2.2 ± 0.3
HP35 0 M	2.8 ± 0.3	3.8 ± 0.4	3.0 ± 0.1	3.7 ± 0.7	3.8 ± 0.1
HP35 4 M	5.1 ± 0.3	2.1 ± 0.1	3.0 ± 0.1	2.3 ± 0.7	2.6 ± 0.1
HP35 6 M	4.8 ± 0.3	2.2 ± 0.1	3.1 ± 0.1	2.0 ± 0.4	2.6 ± 0.1
PheCN water	5.8 ± 0.1	1.8 ± 0.1	2.0 ± 0.1	2.1 ± 0.2	-
PheCN 0 M	4.7 ± 0.1	2.3 ± 0.1	3.1 ± 0.1	2.9 ± 0.5	2.1 ± 0.1
PheCN 4 M	3.9 ± 0.2	2.7 ± 0.1	3.2 ± 0.1	2.3 ± 0.3	2.3 ± 0.1
PheCN 6 M	4.4 ± 0.2	2.4 ± 0.1	3.2 ± 0.1	2.4 ± 0.3	2.1 ± 0.1

viscosity, both shown in Fig. 5*B*, are very similar although not identical. Within the experimental errors, the only significant difference is that the peptide has a larger static component.

Because CN is exposed completely to the solvent in PheCN, its spectral diffusion is expected to be dominated by that of the solvent. For PheCN in water, there is a single decay constant of 2.1 ps and no static component, which is quite close to the slowest time constant of bulk water spectral diffusion (43). When glycerol is added, the dynamics slow, almost certainly due to the increased viscosity.

The fact that the CLS data and the FFCF parameters for the unfolded HP35-$(CN)_2$ in 6 M GuHCl reported by the CN probes are very similar to those of PheCN in the same solvent indicates that dynamics are also dominated by those of the solvent. This observation suggests that the phenylalanine residues that were enclosed by the peptide in a hydrophobic core and, therefore, protected from direct interaction with the solvent, become exposed to the solvent following denaturation. However, the larger value of Δ_s for the HP35 shows that the peptide structure still plays a role in determining the dynamics possibly by partially blocking some access of the solvent to the CN tagged side group. These results are consistent with the unfolded protein assuming a random coil structure as indicated by simulations of HP35 (44).

That the dynamics of HP35-$(CN)_2$ become faster when it is unfolded with GuHCl is in contrast to the findings of a study using 2D IR spectroscopy of CO-bound cytochrome (cyt) *c*. When a thermophilic mutant of cyt *c*, *Ht*-M61A, was denatured by GuHCl, the dynamics slowed down significantly (41). In particular, the static component Δ_s increased upon unfolding by almost a factor of three. Also, the homogeneous component Γ was decreased by half. The reduction in cyt *c* dynamics is attributed to the protein assuming a compact, molten globular state in which the heme-bound CO, the vibrational probe, is still encased by the residual structures of the protein. Indeed, there is an abundance of experimental and theoretical evidences for residual secondary and tertiary structures extant in unfolded cytochrome *c* (1, 45). It is clear from 2D IR experiments that HP35-$(CN)_2$ behaves differently from cyt *c* when it unfolds.

Concluding Remarks

In this work, nitriles bound to HP35 were used as vibrational probes to measure fast dynamics of the peptide in its folded and unfolded configurations and to examine the influence of solvent viscosity. The comparison between the dynamics of the peptide and nitrile-functionalized phenylalanine permitted the dynamics arising from the peptide chain and those from the solvent to be separated. It was shown that an increase in viscosity made a substantial change in the dynamics of the folded peptide. GuHCl was used to unfold the peptide, and the unfolding was verified by CD measurements. The viscosities of the solutions with GuHCl were kept constant by using glycerol as a cosolvent with water. Unfolding the peptide resulted in a substantial increase in the rates of the fast dynamics. The dynamics of the unfolded peptide were very similar but not identical to those of PheCN in the same solvent, suggesting that the peptide CNs become solvent exposed when the protein unfolds.

Materials and Methods

Sample Preparation. The cyano-incorporated villin headpiece 35 (HP35-$(CN)_2$) was synthesized using a solid-phase peptide synthesizer via Fmoc protecting group based chemistry at Stanford University School of Medicine Protein and Nucleic Acid Facility. The amino acid sequence of the peptide was $L_{42}SDEDF_{CN}KAVFGMTRSAF_{CN}ANLPLWKQQNLKKEKGLF_{76}$, where F_{CN} denotes *para*-cyano-L-phenylalanine. The peptide was purified by high-performance liquid chromatography and its purity was checked by electrospray ionization mass spectrometry. PheCN for the optical experiments was obtained from Peptech and used without further purification.

For the optical experiments, samples were dissolved in 50 mM sodium acetate, pH 5.0, with varying concentration of GuHCl. The concentration of GuHCl was checked with calibrated refractive index measurements (46). To control for the effects of the solvent viscosity, glycerol was added to each solvent such that the final viscosity of glycerol-GuHCl-buffer mixture was 2.7 cP (see *SI Text*). For the IR experiments, the final sample concentrations were approximately 16 mM and 120 mM for HP35-$(CN)_2$ and PheCN, respectively, and the path length used was 50 μm.

CD Spectroscopy. CD spectra were measured in the far UV region (200–250 nm, Jasco J810) at 0.5-nm resolution. A 2-mm path length quartz cell was used. The concentration of HP35-$(CN)_2$ sample was approximately 25 μM in various concentrations of GuHCl and glycerol, all in sodium acetate buffer (pH 5.0). The unfolding of the peptide was monitored at 222 nm.

FTIR Spectroscopy. Absorption spectra were obtained with Nicolet 6700 FT IR spectrometer (Thermo Scientific) with 1-cm^{-1} resolution. The CN stretch band occurred at ~2,235 cm^{-1}, where the solvent background absorbance ranged from 0.3 to 0.8 at path length 50 μm depending on the GuHCl and glycerol content, and the CN absorbance intensities were approximately 0.012 and 0.05 for HP35-$(CN)_2$ and PheCN, respectively. The spectra of solvents were also collected for background subtraction, after which baselines were corrected with linear fits to the sloping baseline.

2D IR Vibrational Echo Spectroscopy. The experimental setup and methods of 2D IR vibrational echo spectroscopy are described in detail elsewhere (34, 37). For these experiments, 160 fs-wide mid-IR pulses output from an optical parametric amplifier with spectrum (FWHM 90 cm^{-1}) centered at 2,235 cm^{-1} were used. The energy of each excitation pulse was about 1.2 μJ. The spot size in the sample was ~120 μm.

ACKNOWLEDGMENTS. J.K.C. thanks Yeonju Kwak for helpful discussions. J.K.C., M.C.T., and M.D.F. are grateful to the National Institutes of Health (2-R01-GM061137-09) for support of this research. M.C.T. also thanks the National Institutes of Health for a postdoctoral fellowship.

1. Dill KA, Shortle D (1991) Denatured states of proteins. *Annu Rev Biochem* 60:795–825.
2. Cho JH, Raleigh DP (2009) Experimental characterization of the denatured state ensemble of proteins. *Methods Mol Biol* 490:339–51.
3. Lee MR, Duan Y, Kollman PA (2000) Use of MM-PB/SA in estimating the free energies of proteins: Application to native, intermediates, and unfolded villin headpiece. *Proteins* 39:309–316.
4. Zagrovic B, Pande VS (2006) Simulated unfolded-state ensemble and the experimental NMR structures of villin headpiece yield similar wide-angle solution X-ray scattering profiles. *J Am Chem Soc* 128:11742–11743.
5. Lei HX, Wu C, Liu HG, Duan Y (2007) Folding free-energy landscape of villin headpiece subdomain from molecular dynamics simulations. *Proc Natl Acad Sci USA* 104:4925–4930.
6. Brewer SH, Song BB, Raleigh DP, Dyer RB (2007) Residue specific resolution of protein folding dynamics using isotope-edited infrared temperature jump spectroscopy. *Biochemistry* 46:3279–3285.
7. Glasscock JM, Zhu YJ, Chowdhury P, Tang J, Gai F (2008) Using an amino acid fluorescence resonance energy transfer pair to probe protein unfolding: Application to the villin headpiece subdomain and the LysM domain. *Biochemistry* 47:11070–11076.
8. Wang MH, et al. (2003) Dynamic NMR line-shape analysis demonstrates that the villin headpiece subdomain folds on the microsecond time scale. *J Am Chem Soc* 125:6032–6033.
9. McKnight CJ, Matsudaira PT, Kim PS (1997) NMR structure of the 35-residue villin headpiece subdomain. *Nat Struct Biol* 4:180–184.
10. Chiu TK, et al. (2005) High-resolution X-ray crystal structures of the villin headpiece subdomain, an ultrafast folding protein. *Proc Natl Acad Sci USA* 102:7517–7522.
11. Frauenfelder H, Sligar SG, Wolynes PG (1991) The energy landscapes and motions of proteins. *Science* 254:1598–1603.
12. Parak F, Frauenfelder H (1993) Protein dynamics. *Physica A* 201:332–345.
13. Rella CW, et al. (1996) Vibrational echo studies of protein dynamics. *Phys Rev Lett* 77:1648–1651.
14. Ishikawa H, Kwak K, Chung JK, Kim S, Fayer MD (2008) Direct observation of fast protein conformational switching. *Proc Natl Acad Sci USA* 105:8619–8624.
15. Finkelstein IJ, Ishikawa H, Kim S, Massari AM, Fayer MD (2007) Substrate binding and protein conformational dynamics measured via 2D-IR vibrational echo spectroscopy. *Proc Natl Acad Sci USA* 104:2637–2642.
16. Ganim Z, et al. (2008) Amide I two-dimensional infrared spectroscopy of proteins. *Acc Chem Res* 41:432–441.
17. Bandaria JN, et al. (2010) Characterizing the dynamics of functionally relevant complexes of formate dehydrogenase. *Proc Natl Acad Sci USA* 107:17974–17979.
18. Middleton CT, Woys AM, Mukerhjee S, Zanni MT (2010) Residue-specific structural kinetics of proteins through the union of isotope labeling, mid-IR pulse shaping, and coherent 2D-IR spectroscopy. *Methods* 52:12–22.
19. Kim YS, Hochstrasser RM (2009) Applications of 2d ir spectroscopy to peptides, proteins, and hydrogen-bond dynamics. *J Phys Chem B* 113:8231–8251.

20. Frauenfelder H, McMahon BH, Austin RH, Chu K, Groves JT (2001) The role of structure, energy landscape, dynamics, and allostery in the enzymatic function of myoglobin. *Proc Natl Acad Sci USA* 98:2370–2374.
21. Merchant KA, et al. (2003) Myoglobin-co substate structures and dynamics: Multidimensional vibrational echoes and molecular dynamics simulations. *J Am Chem Soc* 125:13804–13818.
22. Bagchi S, Nebgen BT, Loring RF, Fayer MD (2010) Dynamics of a myoglobin mutant enzyme: 2D-IR vibrational echo experiments and simulations. *J Am Chem Soc* 132:18367–18376.
23. Oh KI, et al. (2008) Nitrile and thiocyanate IR probes: Molecular dynamics simulation studies. *J Chem Phys* 128:154504.
24. Fafarman AT, Webb LJ, Chuang JI, Boxer SG (2006) Site-specific conversion of cysteine thiols into thiocyanate creates an IR probe for electric fields in proteins. *J Am Chem Soc* 128:13356–13357.
25. Webb LJ, Boxer SG (2008) Electrostatic fields near the active site of human aldose reductase: 1. New inhibitors and vibrational stark effect measurements. *Biochemistry* 47:1588–1598.
26. Schultz KC, et al. (2006) A genetically encoded infrared probe. *J Am Chem Soc* 128:13984–13985.
27. Fang C, et al. (2008) Two-dimensional infrared spectra reveal relaxation of the nonnucleoside inhibitor TMC278 complexed with HIV-1 reverse transcriptase. *Proc Natl Acad Sci USA* 105:1472–1477.
28. Urbanek DC, Vorobyev DY, Serrano AL, Gai F, Hochstrasser RM (2010) The two-dimensional vibrational echo of a nitrile probe of the villin HP35 protein. *J Phys Chem Lett* 1:3311–3315.
29. Tang YF, Grey MJ, McKnight J, Palmer AG, Raleigh DP (2006) Multistate folding of the villin headpiece domain. *J Mol Biol* 355:1066–1077.
30. Hu KN, Havlin RH, Yau WM, Tycko R (2009) Quantitative determination of site-specific conformational distributions in an unfolded protein by solid-state nuclear magnetic resonance. *J Mol Biol* 392:1055–1073.
31. Suydam IT, Snow CD, Pande VS, Boxer SG (2006) Electric fields at the active site of an enzyme: Direct comparison of experiment with theory. *Science* 313:200–204.
32. Kawahara K, Tanford C (1966) Viscosity and density of aqueous solutions of urea and guanidine hydrochloride. *J Biol Chem* 241:3228–3232.
33. Rhee YM, Pande VS (2008) Solvent viscosity dependence of the protein folding dynamics. *J Phys Chem B* 112:6221–6227.
34. Park S, Kwak K, Fayer MD (2007) Ultrafast 2D-IR vibrational echo spectroscopy: A probe of molecular dynamics. *Laser Phys Lett* 4:704–718.
35. Kwak K, Park S, Finkelstein IJ, Fayer MD (2007) Frequency-frequency correlation functions and apodization in 2D-IR vibrational echo spectroscopy, a new approach. *J Chem Phys* 127:124503.
36. Kwak K, Rosenfeld DE, Fayer MD (2008) Taking apart two-dimensional infrared vibrational echo spectra: More information and elimination of distortions. *J Chem Phys* 128 204505.
37. Finkelstein IJ, et al. (2007) Probing dynamics of complex molecular systems with ultrafast 2D IR vibrational echo spectroscopy. *Phys Chem Chem Phys* 9:1533–1549.
38. Merchant KA, et al. (2002) Myoglobin-CO conformational substate dynamics: 2D vibrational echoes and MD simulations. *Biophys J* 82:3277–3288.
39. Suydam IT, Boxer SG (2003) Vibrational stark effects calibrate the sensitivity of vibrational probes for electric fields in proteins. *Biochemistry* 42:12050–12055.
40. Ishikawa H, et al. (2007) Neuroglobin dynamics observed with ultrafast 2D-IR vibrational echo spectroscopy. *Proc Natl Acad Sci USA* 104:16116–16121.
41. Kim S, et al. (2008) Native and unfolded cytochrome *c*—Comparison of dynamics using 2D-IR vibrational echo spectroscopy. *J Phys Chem B* 112:10054–10063.
42. Finkelstein IJ, Massari AM, Fayer MD (2007) Viscosity dependent protein dynamics. *Biophys J* 92:3652–3662.
43. Asbury JB, et al. (2004) Dynamics of water probed with vibrational echo correlation spectroscopy. *J Chem Phys* 121:12431–12446.
44. Bowman GR, Ensign DL, Pande VS (2010) Enhanced modeling via network theory: Adaptive sampling of markov state models. *J Chem Theory Comput* 6:787–794.
45. Segel DJ, Fink AL, Hodgson KO, Doniach S (1998) Protein denaturation: A small-angle X-ray scattering study of the ensemble of unfolded states of cytochrome *c*. *Biochemistry* 37:12443–51.
46. Pace CN, Scholtz JM (1997) *Protein Structure: A Practical Approach*, ed TE Creighton (Oxford Univ Press, Oxford, UK), pp 299–321.